

Long-Term Intruding Effects of Acid Rain on Engineering Properties of Primary and Secondary Kaolinite Clays

Zeinab Bakhshipour¹ · Afshin Asadi² · Bujang B. K. Huat¹ · A. Sridharan^{3,4}

Received: 26 January 2016 / Accepted: 1 June 2016 / Published online: 8 July 2016
© Springer International Publishing Switzerland 2016

Abstract In this study, the effects of simulated acid rain (SAR) on the engineering properties of primary and secondary kaolinite clays (PK and SK) were investigated. Tests of consistency limit, compressive strength, compressibility, hydraulic conductivity, and compaction characteristics were conducted to investigate the changes in the physico-chemical and engineering properties of PK and SK clays after being exposed to SAR at different pH levels of 2, 3, 4, 5, and 5.6 and at different fluxes of SAR equivalent to precipitation for 1, 5, 10, and 20 years. In addition, scanning electron microscope (SEM) and energy dispersive X-ray spectroscopy (EDX), zeta potential and atomic adsorption spectroscopy (AAS) studies were conducted to identify the underlying mechanisms involved. The results revealed that for both PK and SK, the low pH value of SAR and higher flux of SAR resulted in a reduction in soil strength, maximum dry density, and increased

compressibility, hydraulic conductivity, liquid limit, and optimum moisture contents. The AAS tests confirmed that reduction of more traced elements in PK and SK specimens when they were infiltrated by the SAR. Also, the formation of relatively a weak structure was observed through the SEM tests. The sensitivity of the PK specimen was higher than that of the SK specimen for SAR intrusion.

Keywords Acid rain · Kaolinite clay · Atterberg limits · Consolidation · Compressive strength · Hydraulic conductivity · Compaction characteristics

Introduction

Acid rain is a secondary pollutant produced when acidic gases dissolve in water. Soils are polluted due to acid rain. This may change the chemistry within the soil environment. Sulfur dioxide (SO₂) and nitrogen oxides (NO_x) are the major sources of acid rain [1–5]. These oxides react in rainwater to produce stronger acids and lower the pH to 4.5 or even 3.0. The engineering properties of soils are significantly influenced by the chemical properties of the medium, termed as “chemical–mechanical coupling” [6]. Many studies have focused on the effects of acid rain on the engineering properties of different soils [6–14]. From the literature, it can be seen that the following chemical and physical processes may describe the effect of acid rain on soil [7, 12]: (I) dissolution and leaching of cations or anions from soil based on their solubility at different pH values; (II) changes in surface electrical properties of the colloidal fraction of soil; (III) absorption of anions in acid rain such as SO₄²⁻, NO₃⁻, and CO₃²⁻ in the soil environment; and (IV) changes in diffuse double layer of clay fraction due to ion exchange and

✉ Zeinab Bakhshipour
bakhshipour.azadeh@gmail.com

Afshin Asadi
afshin.xxxdi@gmail.com

Bujang B. K. Huat
bujang@upm.my

A. Sridharan
sridharanasuei@yahoo.com

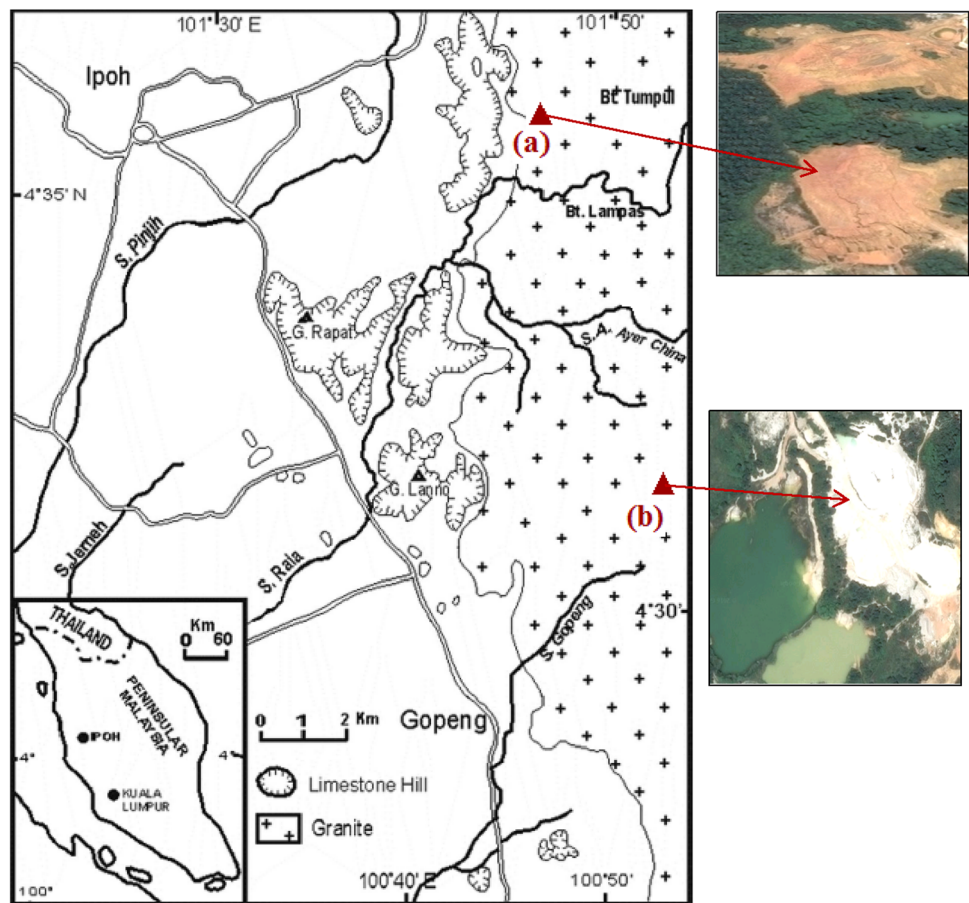
¹ Department of Civil Engineering, Faculty of Engineering, Universiti Putra Malaysia, 43400 Serdang, Selangor, Malaysia

² Housing Research Centre (HRC), Department of Civil Engineering, Faculty of Engineering, Universiti Putra Malaysia, 43400 Serdang, Selangor, Malaysia

³ Indian Institute of Science, Bangalore, India

⁴ Indian National Science Academy, New Delhi, India

Fig. 1 Location of PK and SK soil samples **a** Primary kaolinite, **b** Secondary kaolinite

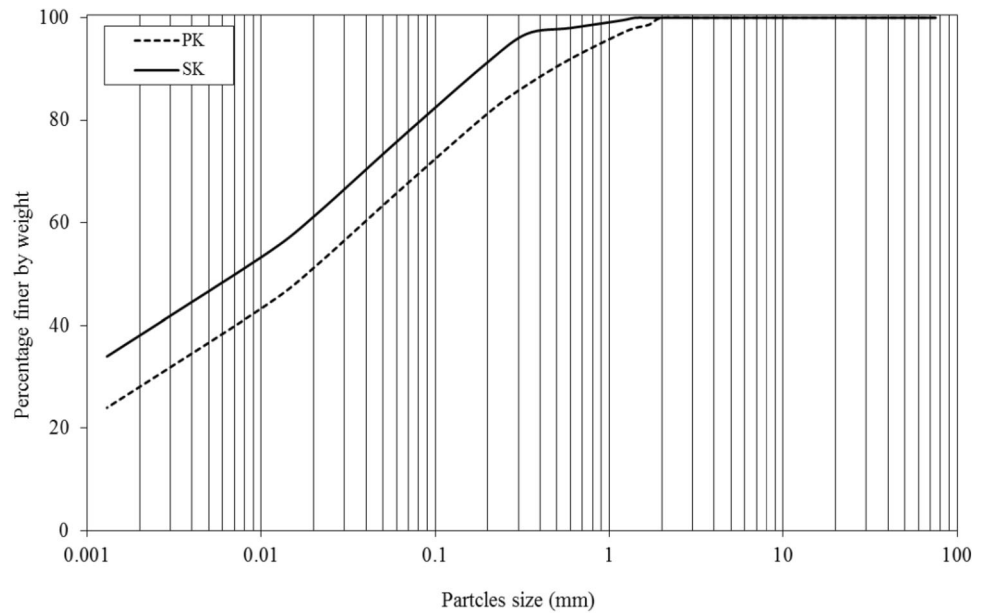


consequent changes in the van der Waals forces acting between the clay particles, which may result in a change in the engineering properties of soil affected by acid rain.

The aforementioned studies have shown that the effects of acid rain on the physico-chemical and engineering properties of soil could be different due to the different properties of the host soil and chemical properties of the pore fluid. Therefore, further studies are needed to elaborate the engineering properties of soil at acidic environmental conditions. Until the end of the 1970s, the problem of acid rain was only confined to European and North American countries. However, increased urbanisation and industrialisation in tropical countries such as Malaysia [15] have provided a basis for the occurrence of acid rain. Malaysia is one of the tropical areas that are beginning to experience the effects of acid rain. In Malaysia, from 1985 to 1992, the mean pH values ranged from 5.0 to 5.7 in the sites not close to industrial areas, and from 4.3 to 5.0 for those near to industrial and densely populated areas [15].

It has long been recognised that in almost all soils of tropical climate areas such as Malaysia, kaolinite clay is one of the predominant clay minerals. Kaolinite clay is a 1:1 alumina silicate mineral composed of one octahedral sheet stacked above one tetrahedral sheet [16]. The two

crystal units comprising one kaolinite clay particle are held together by hydrogen bonds, and the space between the structural layers, therefore, has a fixed dimension [17, 18]. Kaolinite clay with the formula of $\text{Al}_2\text{Si}_2\text{O}_5(\text{OH})_4$ is produced by weathering and typically has low cation exchange capacity (i.e. 2–15 meq/100 g) [16]. Isomorphs substitution within the kaolinite clay crystal is limited, contributing to the low permanent charge. However, kaolinite clay may develop variable or pH-dependent negative charge because of the dissociation of protons for exposed OH^- groups [17, 18]. The surface charge of kaolin in aqueous solutions is always negative, arising in general, directly from Al^{3+} substitution for Si^{4+} in the tetrahedral sheet of the mineral [19]. Kaolinite clay is divided into two broad categories: primary and secondary [16]. Primary kaolinite clay or residual kaolin originates from in situ alteration of rocks by hot fluids, which percolate mainly in pegmatite. Primary kaolinite clay is considered not to have been altered chemically since its deposition and crystallisation as a result of large-scale geological processes [20]. As most primary minerals are formed by tectonic activities, they are inherently unstable in soils and will dissolve [16]. In addition, primary kaolinite clay contains significant amounts of mica, K-feldspar and quartz [21].

Fig. 2 Particle size distribution of PK and SK samples**Table 1** Physical and chemical properties of PK and SK samples

	PK (primary kaolinite)	SK (secondary kaolinite)
Physical properties		
Liquid Limit (LL) (%)	70	44
Plastic Limit (PL) (%)	40	41
Shrinkage Limit (SL) (%)	8	4
Plasticity Index (PI) (%)	30	14
Free Swell Index (%)	33	36
Natural water content (W) (%)	42.32	48.81
Specific Gravity (G_s)	2.53	2.50
Porosity (n) (%)	53.45	57.61
MDD (γ_d) (Mg/m^3)	1.12	1.04
OMC (%)	32	36
Unified Classification of soil	CH (fat clay) clay of high plasticity	CL clay of low plasticity
Chemical properties		
XRF	–	–
Fe_2O_3 (%)	25.98	3.92
SiO_2 (%)	42.01	56.38
Al_2O_3 (%)	23.92	27.27
K_2O (%)	5.20	8.33
pH	4.31	4.27
Cation exchange capacity (meq/100 g)	10.21	8.93

However, secondary minerals form from the decomposition and restructuring of primary minerals or from precipitation reactions involving chemical constituents of primary kaolinite clay released during dissolution [20, 22]. Secondary kaolinite clays are generally characterised by smaller particle size, because the particle size

of primary kaolinite clay decreases during weathering and release of soluble materials [22, 23]. Most secondary kaolinite clays in soils are phyllosilicates: silicate-based minerals having sheets of silicate anions linked to sheets or cations (usually Al) to form a layer [24]. Therefore, secondary kaolinite clay has a more stable structure than

Fig. 3 XRD analysis of original PK and SK soils (k) kaolinite, (q) quartz, (g) goethite, (h) hematite, (k-feldspar) kaolinite-feldspar, (s) smectite, (I) Illite, (ca) calcium

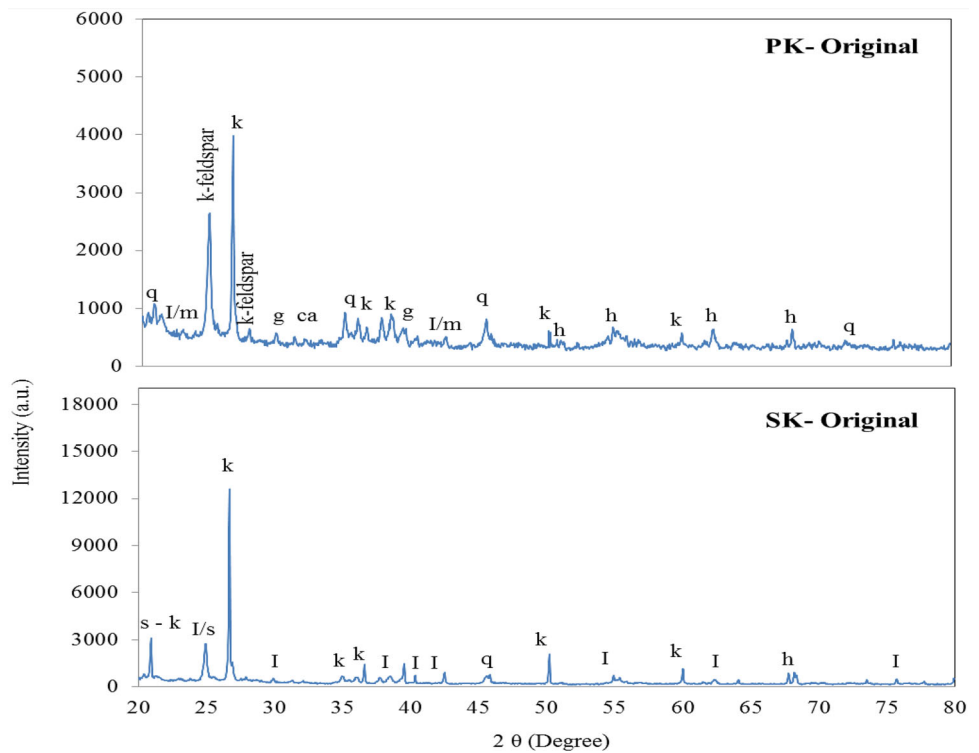
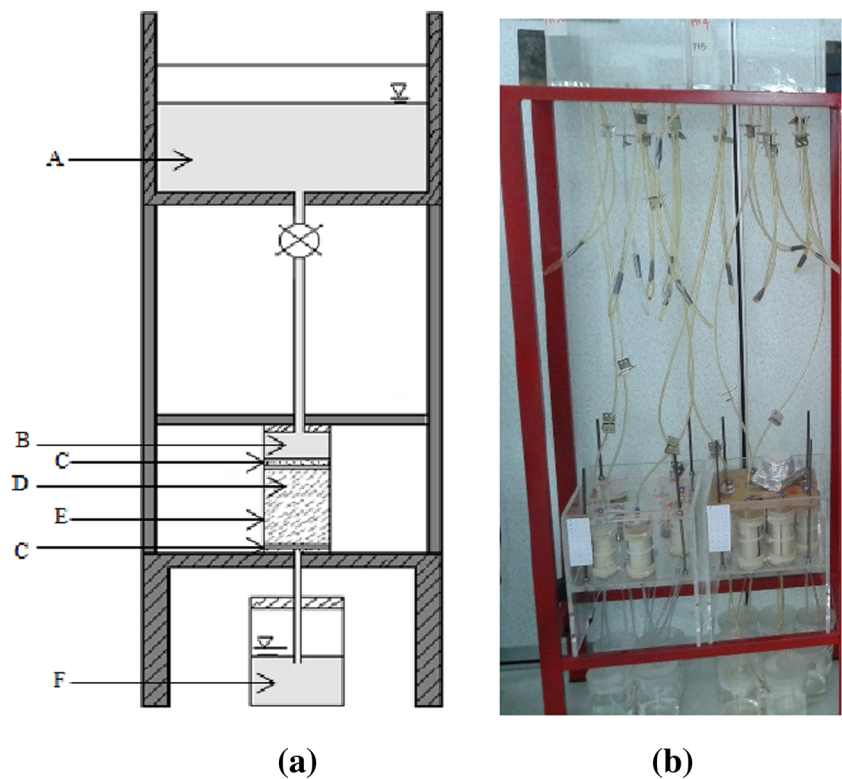


Fig. 4 Exposure setup
a Schematic exposure setup A: SAR tank, B: top cap tank, C: filter paper, D: specimen, E: membrane, F: outflow water,
b Exposure setup in laboratory



that of primary kaolinite clay. Also, secondary kaolinite clay contains significant amounts of illite, vermiculite, and smectite [16].

Most of the soil types in Malaysia contain kaolinite clay as a clay mineral [25]. The climate conditions in Malaysia are characterised by high humidity and particularly

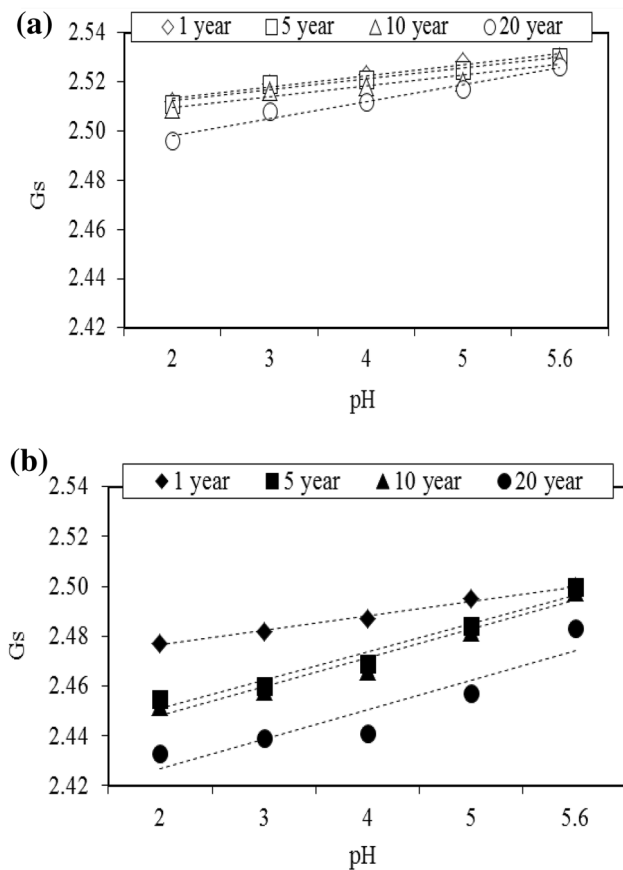


Fig. 5 Specific gravity of soils with respect to pH in flux of SAR 1 year to 20 years **a** PK sample, **b** SK sample

abundant acidic rainfall. Therefore, the effect of acid rain on the physico-chemical and engineering behavior of kaolinite clay is a good context for this study. This study aims to investigate the mechanical effects of simulated acid rain with pH values of 2, 3, 4, 5, and 5.6 on two types of kaolinite clay, including primary and secondary.

Materials and Methods

Soil Properties

Two types of kaolinite clay with different plasticity characteristics were selected. Primary kaolinite (PK) and secondary kaolinite (SK) were obtained from Ipoh (4°35'N 101°46'E) and Bedro (4°32'N 101°54'E) respectively, as shown in Fig. 1. PK and SK were prepared by passing the original kaolinite clay through a 425 μm sieve.

Figure 2 shows the particle size distribution of the specimens. As can be seen from the figure, SK is more fine-grained. This is due to the fact that during transportation, particles are sorted by size and become rounded; therefore, SK was generally formed of more fine-grained and

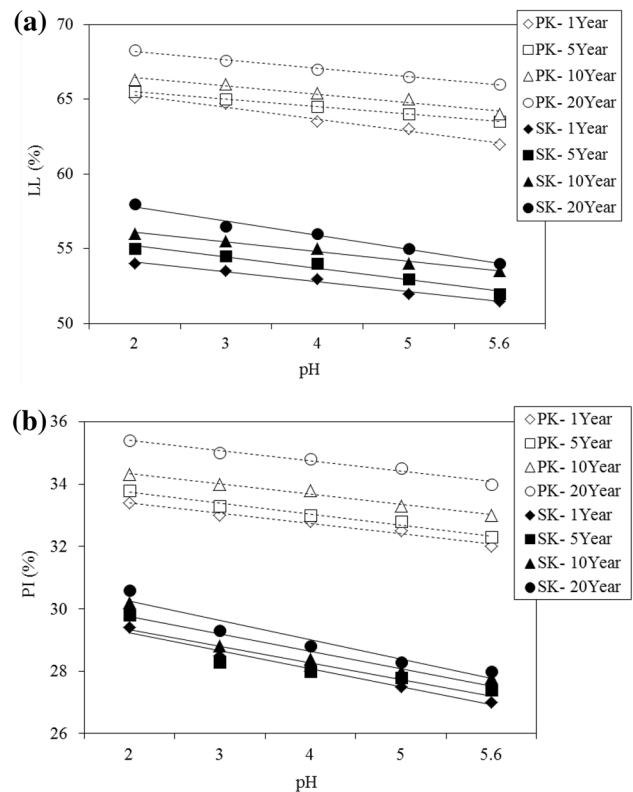


Fig. 6 Consistency limits of PK and SK soils with respect to pH in flux of SAR 1 year to 20 year **a** Liquid limit of PK and SK soils with respect to pH, **b** Plasticity index of PK and SK soils with respect to pH

aggregated particles than PK [26]. The basic properties of these two soils are listed in Table 1. The liquid limit (LL), specific gravity (GS), and water content (WC) were determined according to BSI 1377-2 [27]. The X-ray diffraction (XRD) patterns confirmed the presence of minerals such as mica, K-Feldspar, and quartz in the PK specimen (Fig. 2); moreover, some minerals such as illite and smectite were recorded for the SK specimens (Fig. 3), confirming the purity of the PK and SK soils [16, 21]. X-ray fluorescence (XRF) analyses were carried out to confirm the nature of the clays with a Bruker AXS D8-Advance diffractometer using CuKα radiation. XRF data were collected in both samples and measurements were made using a step-scanning technique with a fixed time of 3 s per 0.028 h.

Simulated Acid Rain Preparation

To investigate the long-term effect of acid rain intrusion, simulated acid rain (SAR) was prepared by adding a certain volume of 0.005 M nitric acid (HNO₃) and sulfuric acid (H₂SO₄) to deionised distilled water. The pH values of the SAR were adjusted to 2, 3, 4, 5, and 5.6. The flux of SAR equivalent to annual precipitation was calculated as flux of

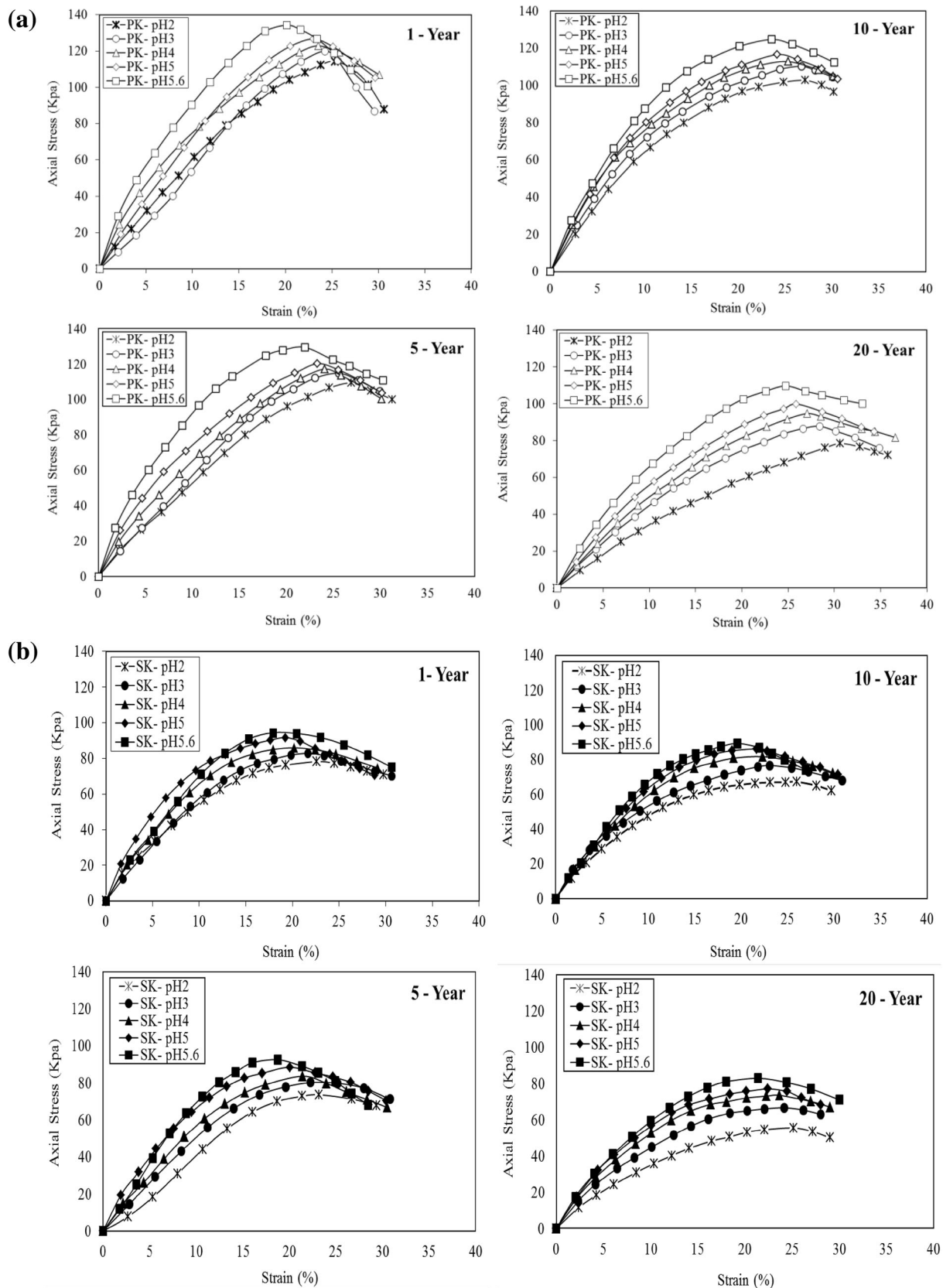


Fig. 7 Stress–strain behaviour of PK and SK samples in flux of SAR 1 year to 20 years, **a** Stress–strain behaviour of PK, and **b** Stress–strain behaviour of SK sample

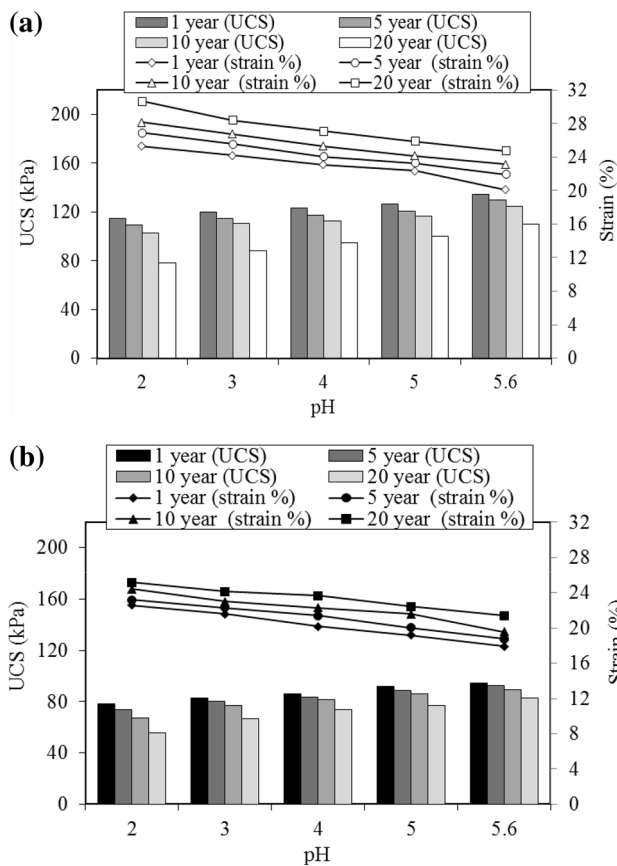


Fig. 8 Devolution of compressive strength of PK and SK samples with respect to pH in flux of SAR 1 year to 20 year **a** Compressive strength of PK, **b** Compressive strength of SK

$SAR = 1/3 R_{ave} A$, where R_{ave} stands for annual average precipitation, and 'A' stands for the cross-sectional area of the specimen. The flux of the SAR was determined based upon the average annual precipitation in Malaysia (i.e. 2400 mm) provided by the Malaysia Meteorological Organisation [25, 26]. It was assumed that one-third of the precipitation will infiltrate into the ground [27]. Therefore, the SAR fluxes equivalent to precipitation for 1, 5, 10 and 20 years were determined to be equal to 1.57, 7.85, 15.70, and 31.4 l, respectively.

Infiltration Tests and Ground Engineering Properties

In order to investigate the effect of SAR on unconfined compressive strength (UCS), the soil specimens were prepared at MDD and OMC using a mini compaction apparatus with a diameter of 50 mm and height of 100 mm, devised by Sridharan and Sivapulliah [28]. Afterward, the soil specimen was extruded and placed into the infiltration cells. The infiltration setup was fabricated as shown in Fig. 4. The setup consisted of transparent PVC pipes with

two different dimensions including an internal diameter of 50 mm, height 100 mm; and internal diameter of 100 mm, height 50 mm. To confine the soil samples, a surrounding membrane was used to keep the soil and two caps at the top and bottom of the specimen, in order to ensure there was no leach out of SAR from the soil. To inject the SAR to the soil, a tank was connected to the top cap using a pipe and control valve. The samples were then infiltrated by different pH levels of the SAR for different fluxes of SAR, equivalent to precipitation for 1, 5, 10, and 20 years.

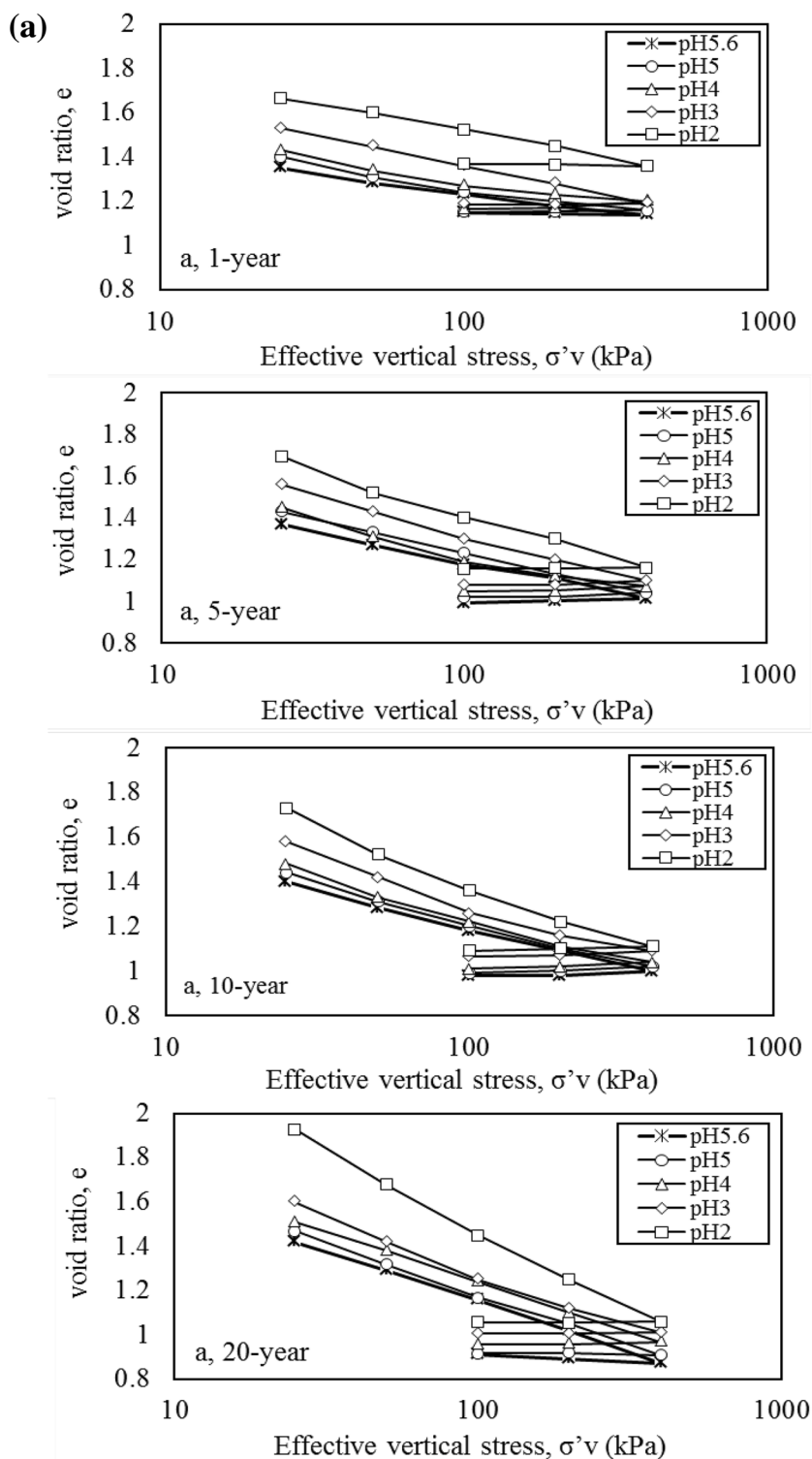
The UCS tests were performed on treated specimens in accordance to BSI 1377-7 [27]. Thereafter, the Atterberg limits of the samples were measured at varying values of pH using the Casagrande method according to BSI 1377-2 [27]. Also, the infiltration setup was slightly modified to measure the hydraulic conductivity by falling head method [29]. Furthermore, the Proctor compaction test was carried out on treated specimens using a mini compaction apparatus devised by Sridharan and Sivapulliah [28]. Moreover, the specific gravity test was determined on PK and SK samples at pH 2, 3, 4, 5, and 5.6 and at different fluxes of SAR equivalent to precipitation for 1–20 years in accordance with BS 1377-2 [27].

In order to investigate the effect of SAR on the compressibility behavior of soil, the soil specimen was prepared at MDD and OMC. Afterward, the soil specimen was extruded and placed into the exposure cell. The exposure cell was similar to that shown in Fig. 3. The sample was then infiltrated by different pH levels of the SAR for different fluxes. Finally, the specimens with diameter 10 cm were carefully cut into smaller specimens with height 20 mm. Consolidation tests were performed in an a one-dimensional oedometer according to BS 1924: Part 2-Sect. 4 [27]. Overburden stress was applied in increments of 25, 50, 100, 200, 400, and 100 kPa, followed by unloading. The compression index C_c , the slope of the virgin compression curve, was computed as: $C_c = (e_{100\text{ kPa}} - e_{400\text{ kPa}}) / (\log(400\text{ kPa}/100\text{ kPa}))$, where "C_c" is compression index and "e" is void ratio.

Zeta Potential Test

In order to prepare the specimens for zeta potential (ζ) measurement at varying values of pH of 2, 3, 4, 5 and 5.6, the PK and SK samples infiltrated by SAR were dried at 80 °C for 48 h. They were then sieved through a No. 100 (150 μm) size sieve. A 15 mg specimen was then transferred into 50 mL aqueous solution, and magnetic stirring bars were subsequently added. The pH adjustments were performed using dilute HNO₃ and H₂SO₄ [30]. The ζ was measured by Malvern Zetasizer 3000HSA (Malvern Instruments, Ltd.) equipped with a microprocessor unit.

Fig. 9 Influence of pH on void ratio-effective vertical stress relationship in flux of SAR
 1 year to 20 year a pH on void ratio-effective vertical stress of PK, **b** pH on void ratio-effective vertical stress of SK

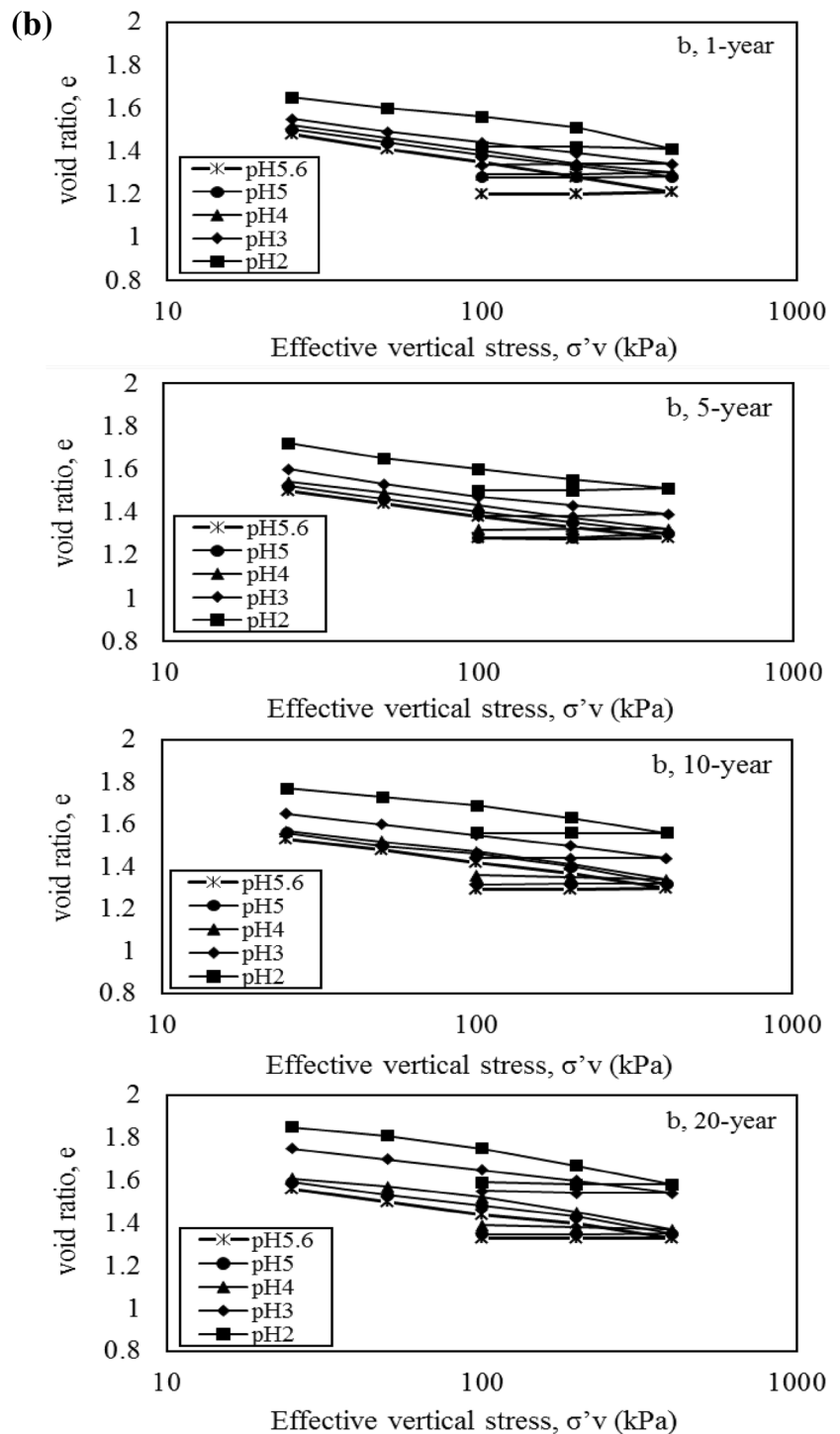


Atomic Adsorption Spectroscopy

The atomic adsorption spectroscopy (AAS) technique was used to measure the concentration of elements (i.e. Al, Fe, Si, K, and Ca) in soil infiltrated by different pH levels of

the SAR for different fluxes of SAR. 0.05 g of soil infiltrated by SAR was oven-dried at 105 °C for 4 h. Afterwards, the soil powders were mixed with 100 ml HCL 65 % (Merck). The aqueous solution was then thoroughly stirred for 2 h. Finally, the traced elements were measured

Fig. 9 continued



by AAS. Also, the concentration of elements in the outflow water leached from the PK and SK was measured with the same technique.

In addition, the water extraction method was used to measure the basic soluble cations of soil infiltrated by different pH levels of the SAR for the different fluxes. The extracted solution was then analyzed by AAS for the soil cations [31].

Scanning Electron Microscope and Energy Dispersive X-ray Spectroscopy

Scanning electron microscope (SEM) analyses and energy dispersive X-ray spectroscopy (EDX) were carried out to understand the underlying mechanisms of the effects of acid rain on the studied soils, before and after the treatment of soil by SAR at pH 2 for different fluxes of SAR.

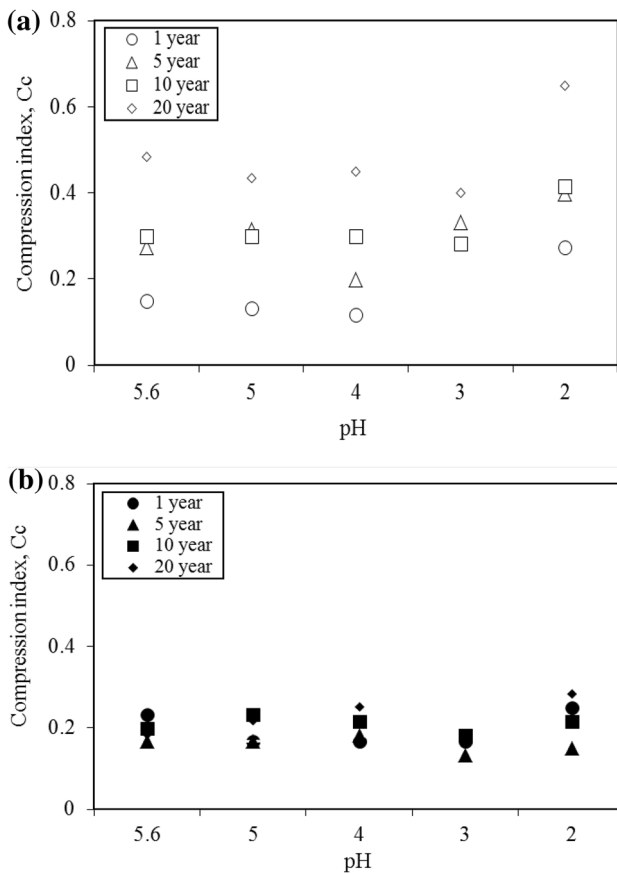


Fig. 10 Influence of pH on compression index in flux of SAR 1 year to 20 year **a** PK sample, **b** SK sample

Results and Discussion

Specific Gravity Results

Specific gravity calculations [27] were performed by determining the ratio of slurry weight to water weight required to fill a graduate cylinder. Figure 5 shows the ranges of variation of G_s in both samples. It is seen that the G_s decreased for both the PK and SK specimens when the pH value decreased and the flux of SAR increased. The highest G_s value in both kaolinite clays was recorded at pH 5.6 when both samples were infiltrated by a flux of SAR equivalent to precipitation for 20 years. It was observed that the effect of the flux of SAR for the PK specimen was much more than that of the SK specimen.

Atterberg Limits Results

Figure 6a shows the result of LL of the PK and SK samples, with the effect of different pH values for different fluxes of SAR. As can be seen from the figure, LL increased with a decrease of pH value for all fluxes of SAR and all pH levels. The highest LL of 68 and 58 % were

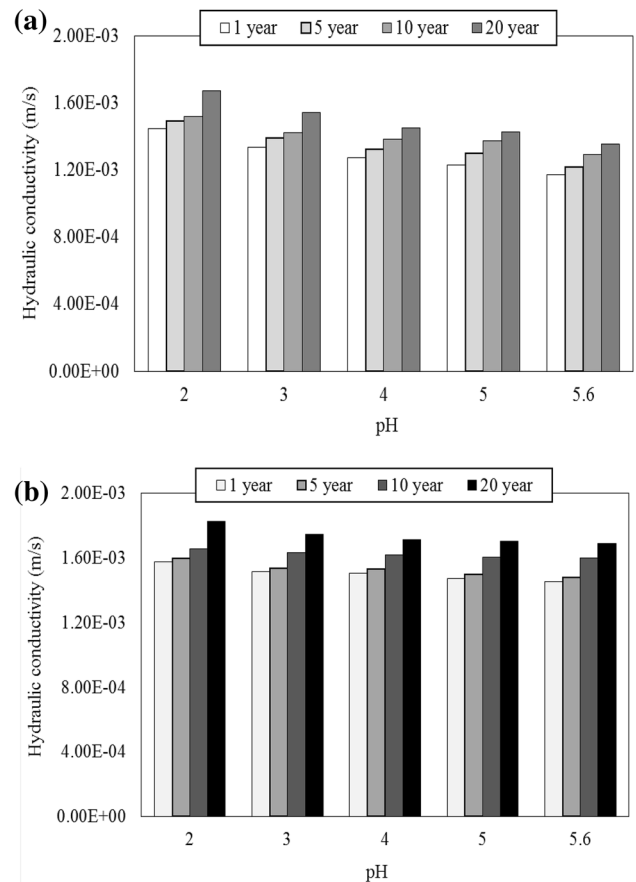


Fig. 11 Hydraulic conductivity of PK and SK soils with respect to pH **a** Hydraulic conductivity of PK in flux of SAR 1 year to 20 years, **b** Hydraulic conductivity of SK in flux of SAR 1 year to 20 years

recorded for PK and SK at pH 2, when both samples were infiltrated by a flux of SAR equivalent to precipitation for 20 years. It should be noted that the range of variations of LL in the PK soil is slightly greater than that of the SK samples.

Figure 6b shows the variation of plasticity index (PI) in both samples. It can be seen that the PI increased for both samples when the pH value decreased and the flux of SAR increased. The highest PI value was recorded at pH 2 when both samples were infiltrated by a flux of SAR equivalent to precipitation for 20 years. It was also observed that the effect of the flux of SAR for the PK specimen was much greater than that of the SK specimen.

Unconfined Compression Results

Figure 7 shows the stress–strain behaviour of the PK and SK specimens influenced by SAR for the different fluxes. As can be seen from the figure, the PK and SK specimens infiltrated by a flux of SAR equivalent to precipitation for 1 year at pH 2 exhibited peak strength of 114 and 78 kPa at

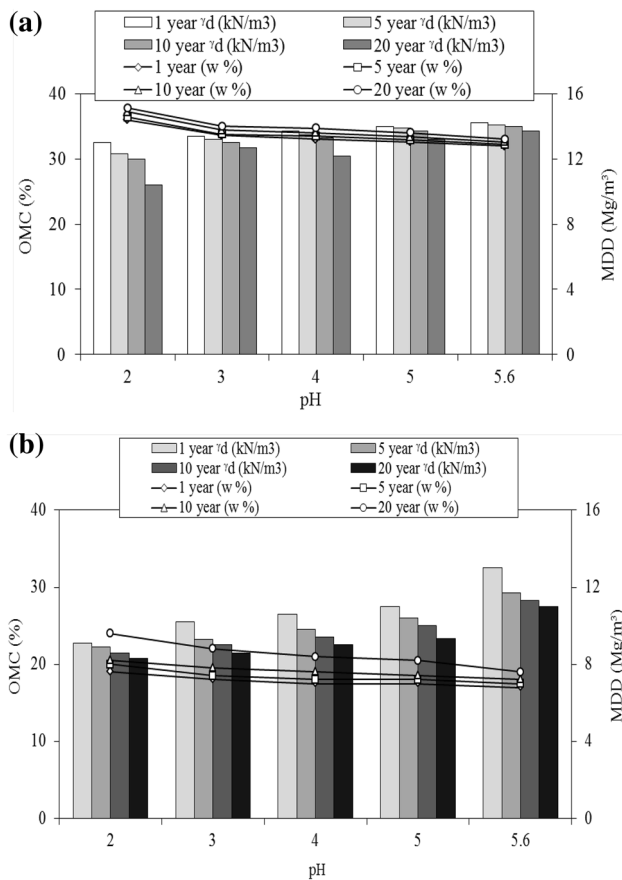


Fig. 12 Compaction characteristics of PK and SK soils with respect to pH **a** Compaction characteristics of PK in flux of SAR 1 year to 20 years, **b** Compaction characteristics of SK in flux of SAR 1 year to 20 years

failure strains of 25 and 22 % respectively. However, the peak strength decreased to 78 and 55 kPa at failure strains of 30 and 25 % respectively, as the flux of the SAR increased to that of 20 years at pH 2. Similar behaviour for the peak strength was observed for the PK and SK samples infiltrated by SAR at different pH levels, when the fluxes of the SAR increased to that of 20 years. The results showed that the rate of strength loss for the PK sample was higher than that of the SK sample as the fluxes of the SAR increased from 1 year to 20 years.

Figure 8 shows the devolution of compressive strength and strain at failure with respect to pH level of SAR for the PK and SK samples, respectively. The highest rate of strength loss was recorded at about 78 and 55 kPa for the PK and SK samples, respectively, when the specimen was infiltrated by SAR at pH of 2 with a flux equivalent to 20 years. Furthermore, in both the PK and SK samples, the strain at failure increased as the pH level decreased or as the flux of SAR increased. The highest failure strains for both PK and SK samples infiltrated with a flux of SAR equivalent to 20 years were recorded as 30 and 25 %, respectively.

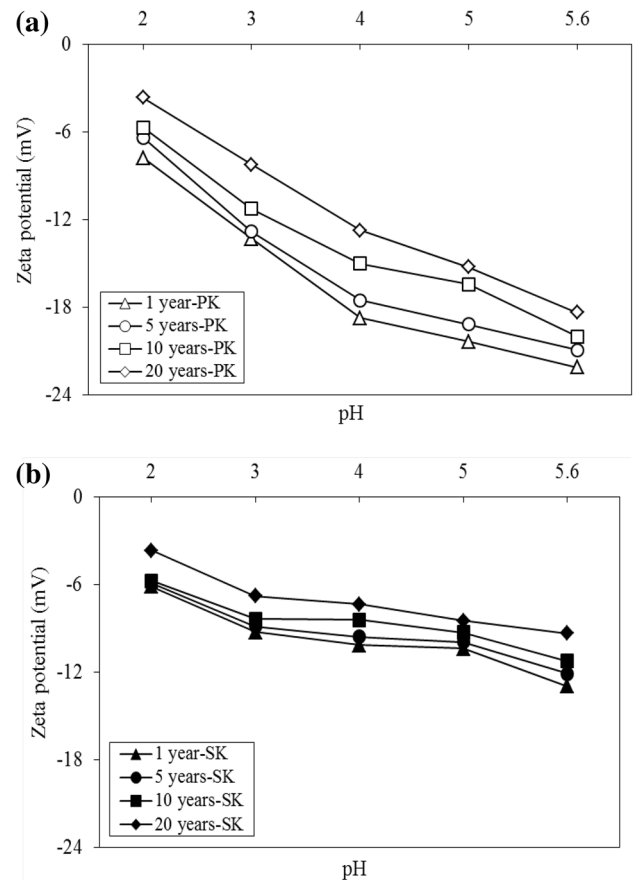


Fig. 13 Zeta potential of soils with respect to pH in flux of SAR 1 year to 20 years **a** PK sample, **b** SK sample

respectively. The results revealed that for both the PK and SK samples, a lower pH level of the SAR and higher fluxes of SAR could change the behaviour of clay minerals to be more brittle and with a lower compressive strength. However, the rate of change for the PK sample was observed to be higher than that of the SK sample.

One-Dimensional Consolidation Results

The laboratory results indicated that the SAA had a strong influence on the compressibility behaviour of the specimens. It was observed that the uppermost virgin compression curve in PK and SK had the lowest pH value of 2. The initial void ratio of PK and SK increased as the pH decreased or the flux of SAR increased. For instance, in PK and SK at pH 2 with the flux of SAR for 20 years, the value of void ratio was 1.93 and 1.85, respectively. On the other hand, for the same pH at 1 year, the initial void ratios were 1.67 and 1.63 respectively, which may be the result of the longer exposure to the SAR (Fig. 9).

Figure 10 shows the evolution of compression index, C_c , at different pH levels and at for a variety of fluxes of

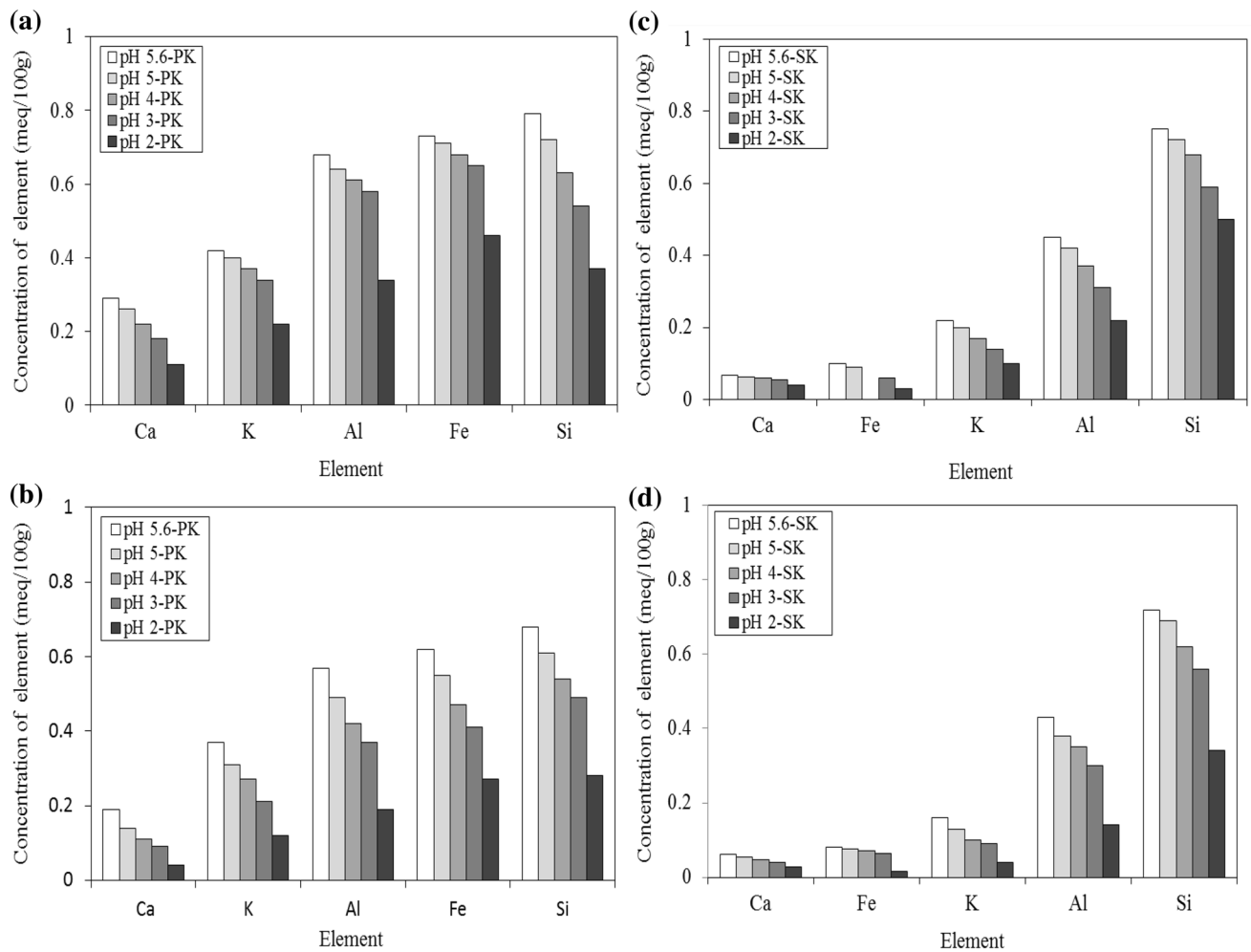


Fig. 14 AAS analysis of soil before and after filtration by SAR in flux of 1 year and 20 year **a** PK-1 year, **b** PK-20 years, **c** SK-1 year, and **d** SK-20 years with respect to pH

SAR for 1, 5, and 20 years in the PK and SK specimens. Figure 10 shows that C_c can significantly increase as the environment becomes more acidic. For instance, the highest value of C_c was recorded to be about 0.64 and 0.28 for the PK and SK samples, respectively, when the specimen was infiltrated by SAR at pH of 2 with the flux equivalent to 20 years. It is clear from the figures that the effect of low pH values had a more pronounced influence on C_c for both specimens. It was observed that the increase in compressibility behaviour was in agreement with the increase in LL and the reduction in compressive shear strength of both the PK and SK specimens.

Hydraulic Conductivity Results

The change in hydraulic conductivity values against the permeated fluxes of SAR is shown in Fig. 11. The results confirmed that the hydraulic conductivity increased with a

decrease in pH value and increase of fluxes of SAR. The hydraulic conductivity of both the PK and SK specimens increased by 15 and 13 %, respectively, at pH 2, when the samples were infiltrated by a flux of SAR equivalent to precipitation for 20 years, which is consistent with the results of unconfined compressive strength. The increase in hydraulic conductivity of both samples could be attributed to the small increase of the void ratio (i.e. a decrease in the dry density) and possibly due to decrease in diffuse double layer thickness during the test.

Compaction Results

The PK and SK specimens initially showed an MDD and OMC of 1.12 Mg/m^3 and 32 %, and 1.04 Mg/m^3 and 36 % respectively (see Table 1). Figure 12 shows the compaction characteristics of the PK and SK specimens influenced by different pH levels and different fluxes of SAR.

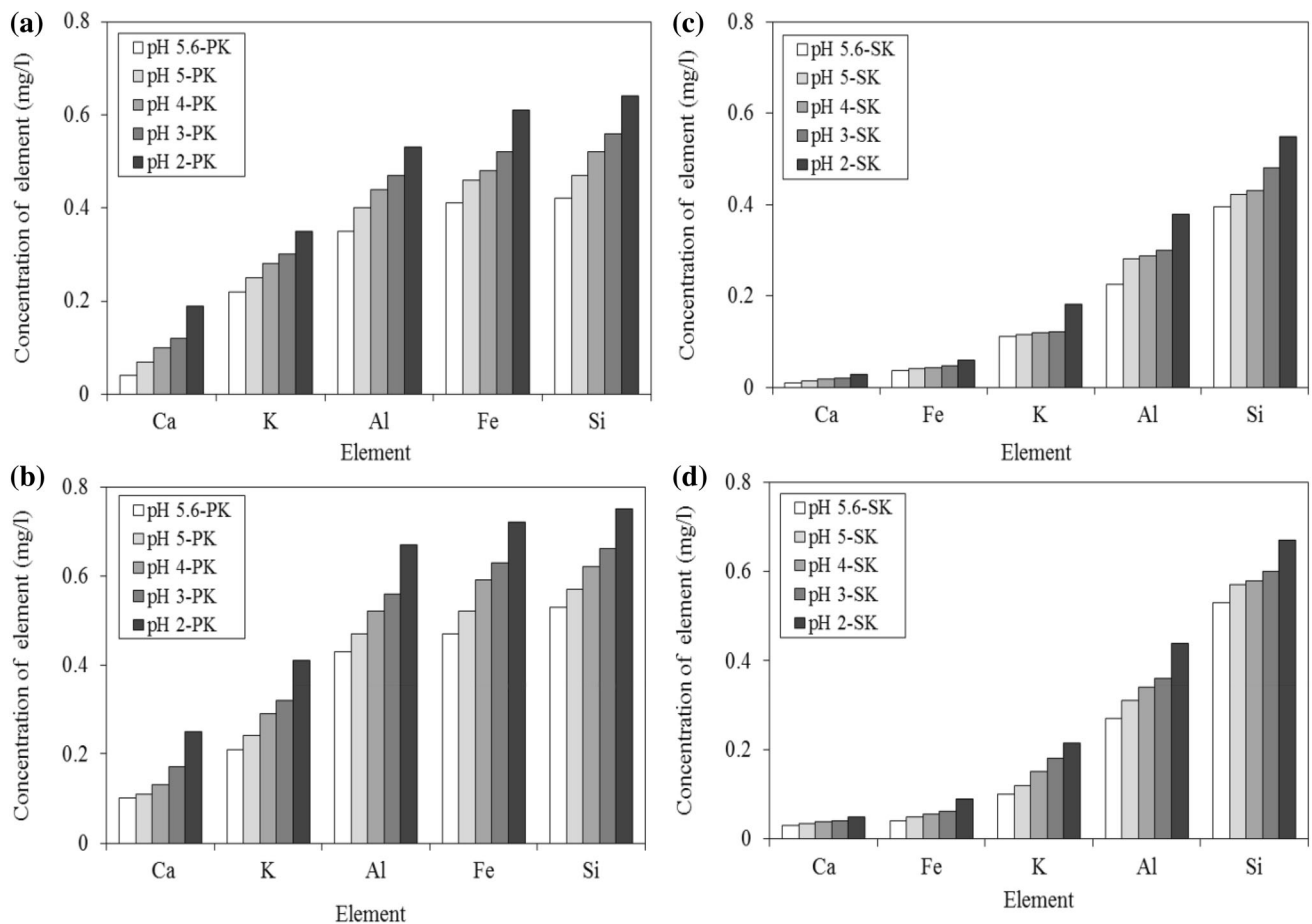


Fig. 15 AAS analysis of leachate from **a** PK-1 year, **b** PK -20 years, **c** SK -1 year, **d** SK- 20 years, with respect to pH

As can be seen from the figure, infiltration of SAR into both specimens led to decreased MDD and increased OMC. The lowest MDD and the highest OMC were observed when the specimens were infiltrated by a flux of SAR equivalent to precipitation for 20 years at pH 2. It was also observed that the PK specimen showed slightly higher changes compared to the SK specimen. This behaviour is consistent with the Atterberg limits behaviour (Fig. 5).

Zeta Potential Results

Figure 13 indicates the zeta potential (ζ) of specimens in the presence of SAR at different pH values. As can be seen from the figure, ζ of PK and SK decreased as the pH dropped from 5.6 to 2. It should be noted that the surface charge of kaolinite clay is pH-dependent [32–34]. The pH-dependent negative surface charge of kaolinite clay can be attributed to the dissociation of OH^- groups on clay edges [33]. As can be seen, the effect of pH on ζ of PK was slightly higher than for the SK specimens.

From clay colloid chemistry [35], it is also known that this ion exchange process would lead to an increase in equivalent diffuse double layer thickness. Nevertheless,

this process is likely to have fewer effects on mechanical changes in both the PK and SK samples. This can be explained by the fact that kaolinite clay does not develop sufficient diffuse double layer repulsive force to influence the changes in the engineering properties [13, 14, 36].

The zeta potential, ζ , measurements showed that the surface charge of both minerals was pH-dependent (Fig. 13). It was confirmed that, under the effects of SAR, the zeta potential of both minerals decreased. This indicates a relatively flocculated fabric for the kaolinite clay particles with dominant edge-to-face particle associations [14] that resulted in a reduction in soil strength and, consequently, the observed changes in Atterberg limits and compaction characteristics.

Results from Atomic Adsorption Spectroscopy

The atomic adsorption spectrometry (AAS) analysis in Fig. 14 shows the elemental concentrations of soil before and after filtration by SAR. The results show that the concentration of trace elements in PK and SK significantly decreased when the specimens were influenced by different fluxes of SAR at different pH levels. In order of abundance

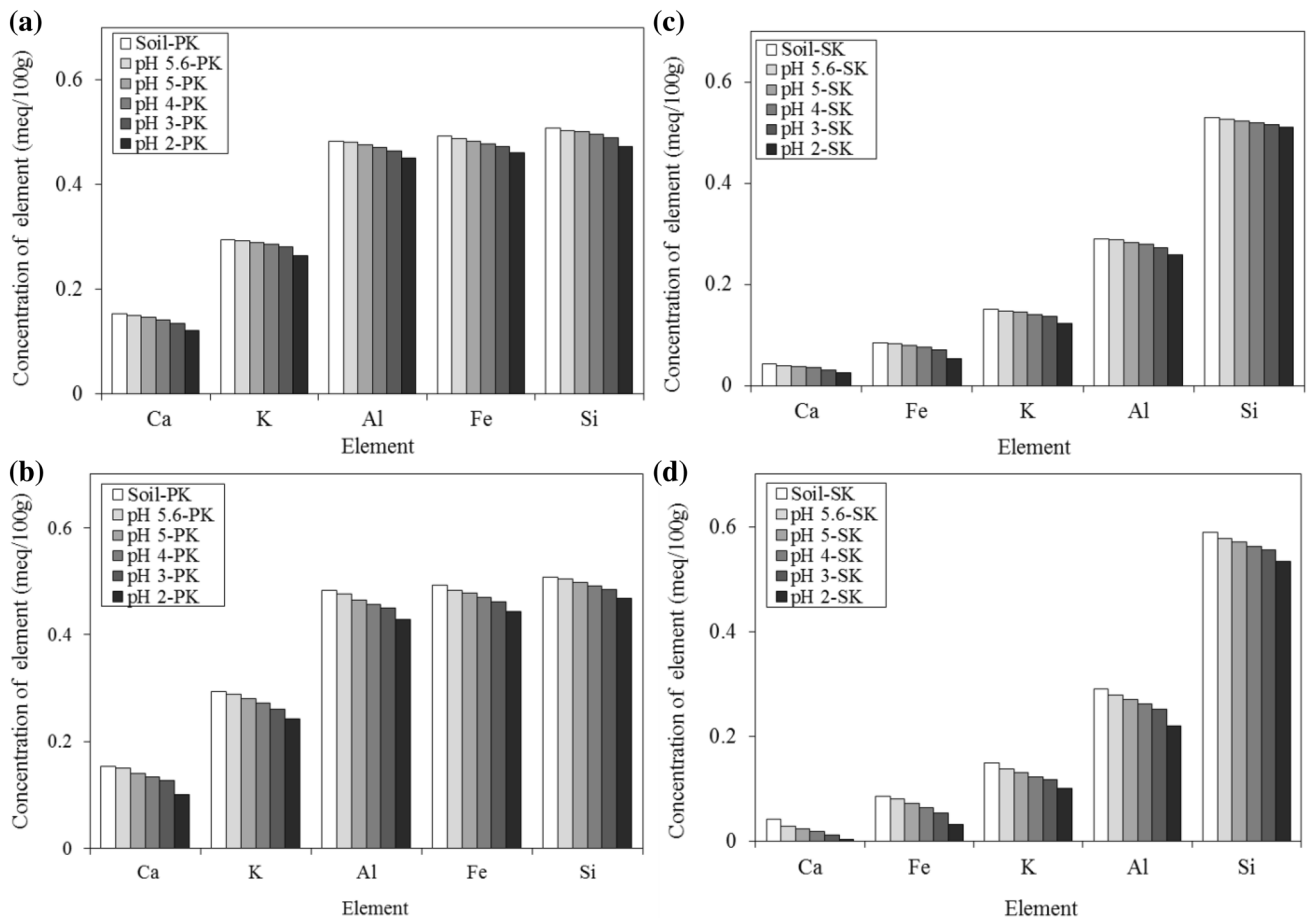


Fig. 16 Ion-soluble analysis of soil before and after filtration by SAR **a** PK -1 year, **b** PK -20 years, **c** SK-1 year, and **d** SK-20 years, with respect to pH

in the PK and SK specimens (see Table 1), from most to least, the major constituents were: Si, Fe, Al, and K; and Si, Al, K, and Fe, respectively. The concentration of Fe, Al, and Si in PK and SK, for example, decreased by around 0.46, 0.34 and 0.37 %; and 0.03, 0.22, and 0.05 % respectively, when the soils were infiltrated by a flux of SAR equivalent precipitation for 1 year at pH 2. In particular, the greatest reduction in the concentration of Fe and Al was observed for PK and SK when the specimens were infiltrated by a flux of SAR equivalent to precipitation for 20 years at pH 2. A comparison between the PK and SK specimens shows that both clay minerals had low pH and high potential leaching rates, due to their having low CEC and a lack of basic chemicals; consequently, the effects of SAR were pronounced due to the lower buffering capacity of the soils [37]. It is believed that the movement of SAR through the PK and SK soils dissolves most of the elements, leaching them out of the samples in the infiltration test.

Figure 15 shows the SAS analysis of outflow fluid leached from PK and SK. As can be seen, there was a general increase in the sum of total cations as a result of increasing the flux and decreasing the pH level of the SAR. The results indicate a correspondence between the variation of the elemental concentrations of soil and the cations in outflow fluid leached from PK and SK. The study of the test results of both clays show that the concentration of elements leached from PK and SK depended on the types of the element, pH and flux of SAR.

Figure 16 shows the concentration of soluble cations before and after infiltration by SAR. As can be seen, there was a general decrease in the amounts of soluble ions between particles, as a result of increasing the flux and also decreasing the pH level of the SAR. The results showed that the greatest reduction in the concentrations of Fe and Al was observed for PK and SK when the minerals were infiltrated by a flux of SAR equivalent to precipitation for 20 years at pH 2.

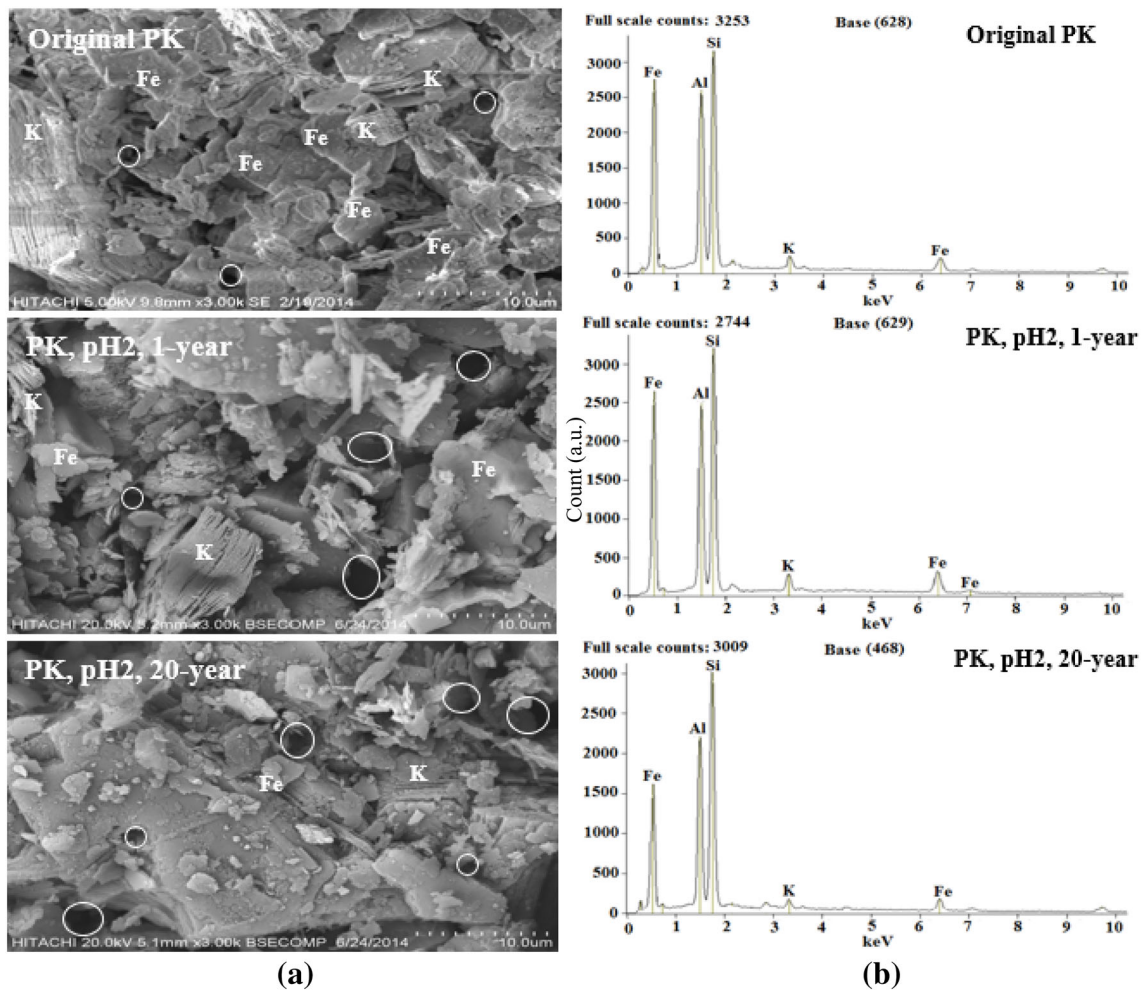


Fig. 17 SEM and EDX analyses of PK in original conditions and pH 2 in flux of SAR 1 year to 20 years **a** SEM images, **b** EDX images

When the specimens became acidic, the hydrogen ions (H^+) from SAR engage in an exchange process with the cations present. Due to its superior position in the Hofmeister series, H^+ would replace Fe^{3+} and Al^{3+} . Figures 13 and 14 clearly confirmed that most of the traced elements and cations, including Fe^{3+} and Al^{3+} , were leached out from the matrix when the pH decreased. Moreover, SAR consisted of a mixture of nitric acid and sulfuric acid, which is known as a strong oxidiser due to the electron donor property of NO_3^- and SO_4^{2-} ions in the acidic media, causing a conversion from Fe^{2+} to Fe^{3+} , and expediting the leaching of Al^{3+} and Fe^{3+} in the acidic media. A decrease in iron and aluminum content means the destruction of soil structure: consequently, the shear strength, MDD, and specific gravity decreased, while the OMC, PI, and LL increased.

EDX and SEM Analysis

Figures 17 and 18 show SEM and EDX analyses of the PK and SK samples before and after treatment at pH 2 of the

SAR for different fluxes of SAR equivalent to precipitation for 1 and 20 years. As can be seen from the SEM results, the PK and SK samples consisted of some large particle packs; clay particles cohered together in the presence of water, therefore forming large particle packs and a densified soil matrix. After SAR treatment, some large spaces between clay particles appeared and disintegration increased as the flux of SAR increased from 1 to 20 years.

The EDX results revealed that after SAR treatment, most of the minerals were leached out from the clay particles due to the infiltration of specimens by SAR. Very large spaces between clay particles in the specimens in the SEM results are attributed to the washing and leaching out of Al^{2+} , Fe^{3+} , Si^{2+} , and K^+ from the clay particles during infiltration. The original PK had a high content of iron and aluminum: about 2800 and 2600 count (a.u.) respectively. The results illustrated that the Fe and Al content decreased to 64 and 72.1 % in the PK sample, respectively. The presence of free iron oxide and aluminum oxide has an important role in cementation in clay particles, which

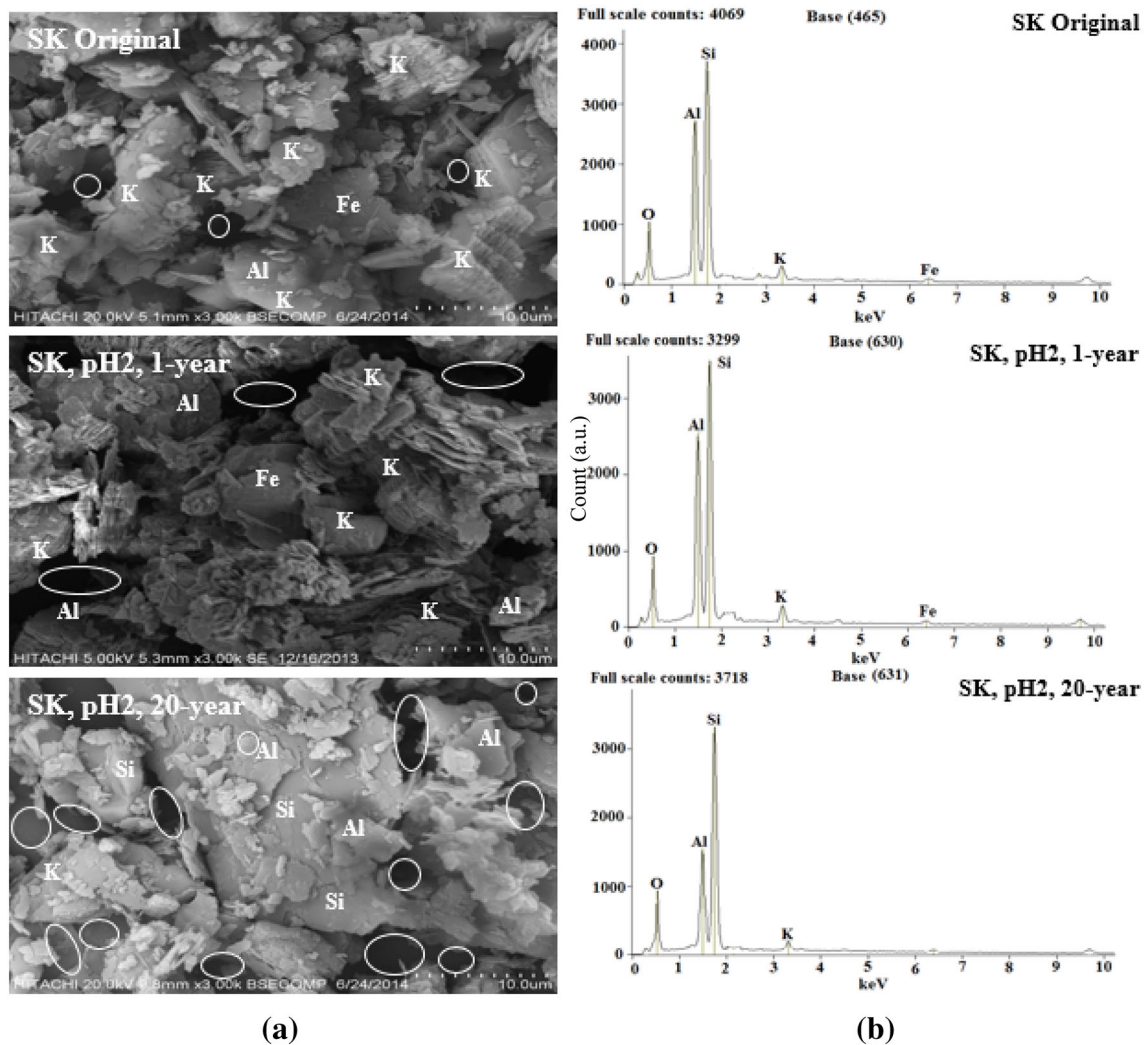


Fig. 18 SEM and EDX analyses of SK in original conditions and pH 2 in flux of SAR 1 year to 20 years **a** SEM images, **b** EDX images

increased the bonding between the finer particles of soils [38–40]. This process destroyed the bonds between clay particles/aggregates: significant changes in mineral structure occurred due to the dissolution of alumina and silica from the PK and SK soils, forming “loose” structures with larger voids. Consequently, the shear strength decreased.

Conclusions

The results revealed that for both primary kaolinite clay (PK) and secondary kaolinite clay (SK), the low pH value of simulated acid rain (SAR) and higher flux of SAR resulted in a reduction in soil strength and maximum dry density in compaction tests, and increased compressibility, hydraulic conductivity, liquid limit, and optimum moisture content. The results showed that the effect of acidic environment were higher for PK specimens than those of the SK specimens. The greatest

number of intrusion effects was observed when the pH value was 2 and the flux of SAR was equivalent to precipitation for 20 years. The atomic adsorption spectroscopy (AAS) and energy dispersive X-ray spectroscopy (EDX) results confirmed that most of the traced elements and metallic cations, including Fe^{3+} and Al^{3+} , were leached out from the soil matrix when the pH decreased. Also, scanning electron microscope analyses confirmed the formation of a relatively weak structure after acid rain treatment. It was concluded that acid rain led to important changes on ground engineering properties of kaolinite clays.

Acknowledgments The authors sincerely give thanks to the University Putra Malaysia and Fundamental Research Grant Scheme (FRGS/5524133) entitled ‘acid rain intrusion effects and slope failure phenomena and mechanisms’ for financial support for this research. Moreover, sincere thanks are due to Dr. Hossein Jahangirian from the USA who shared some particularly fruitful discussions with us.

References

- Denman KL, Brasseur G, Chidthaisong A, Ciais P, Cox PM, Dickinson RE, Hauglustaine D, Heinze C, Holland E, Jacob D (2007) Couplings between changes in the climate system and biogeochemistry. *Clim Change* 2007:541–584
- Galloway JN (1989) Atmospheric acidification: projections for the future. *Ambio* 161–166
- Kato N, Akimoto H (1992) Anthropogenic emissions of SO₂ and NO_x in Asia: emission inventories. *Atmos Environ A* 26(16):2997–3017
- Streets D, Waldhoff S (2000) Present and future emissions of air pollutants in China: SO₂, NO_x, and CO. *Atmos Environ* 34(3):363–374
- Menon S, Denman KL, Brasseur G, Chidthaisong A, Ciais P, Cox PM, Dickinson RE, Hauglustaine D, Heinze C, Holland E (2007) Couplings between changes in the climate system and biogeochemistry. Ernest Orlando Lawrence Berkeley National Laboratory, Berkeley
- Santamarina J, Klein K, Wang Y, Prencke E (2002) Specific surface: determination and relevance. *Can Geotech J* 39(1):233–241
- Benna M, Kbir-Arighuib N, Clinard C, Bergaya F (2002) Cardhouse microstructure of purified sodium montmorillonite gels evidenced by filtration properties at different pH. *Adsorption and Nanostructure*. Springer, Berlin, pp 204–210
- Brandenburg U, Lagaly G (1988) Rheological properties of sodium montmorillonite dispersions. *Appl Clay Sci* 3(3):263–279
- Gajo A, Maines M (2007) Mechanical effects of aqueous solutions of inorganic acids and bases on a natural active clay. *Géotechnique* 57(8):687–699
- Gori U (1994) The pH influence on the index properties of clays. *Bull Int Assoc Eng Geol* 50(1):37–42
- Gratchev IB, Sassa K (2009) Cyclic behavior of fine-grained soils at different pH values. *J Geotech Geoenviron Eng* 135(2):271–279
- Jozefaciuk G, Bowanko G (2002) Effect of acid and alkali treatments on surface areas and adsorption energies of selected minerals. *Clays Clay Miner* 50(6):771–783
- Sridharan A, El-Shafei A, Miura N (2002) Mechanisms controlling the undrained strength behavior of remolded Ariake marine clays. *Mar Georesour Geotechnol* 20(1):21–50
- Sridharan A, Rao S, Murthy N (1988) Liquid limit of kaolinitic soils. *Geotechnique* 38(2):191–198
- Ayers G, Peng LC, Fook LS, Kong CW, Gillett R, Manins P (2000) Atmospheric concentrations and deposition of oxidised sulfur and nitrogen species at Petaling Jaya, Malaysia, 1993–1998. *Tellus B* 52(1):60–73
- So HB, Lal R (2002) *Encyclopedia of soil science*. Taylor & Francis, New York
- Tan K, Bartlett RJ (1994) Principles of soil Chemistry. *Soil Sci* 157(5):330
- Dixon JB, Schulze DG (2002) Soil mineralogy with environmental applications. Soil Science Society of America Inc., Madison
- Bolland MDA, Posner A, Quirk J (1976) Surface charge on kaolinites in aqueous suspension. *Soil Res* 14(2):197–216
- Evans GO (1992) Principles of acarology, vol 18. CAB International, Wallingford
- Bloodworth A, Highley DE, Mitchell C (1993) Industrial minerals laboratory manual: Kaolin
- Scorzelli G, Paoluzzi A, Pascucci V (2008) Parallel solid modeling using BSP dataflow. *Int J Comput Geom Appl* 18(05):441–467
- Tan KH (2010) Principles of soil chemistry. CRC Press, Boca Raton
- Norton R (1985) Aspects of the biology and systematics of soil arachnids, particularly saprophagous and mycophagous mites. *Quaest Entomol* 21:523–541
- Shamshuddin J, Anda M (2008) Charge properties of soils in Malaysia dominated by kaolinite, gibbsite, goethite and hematite. *Bull Geol Soc Malays* 54:27–31
- Scorzelli R, Bertolino L, Luz A, Duttine M, Silva F, Munayco P (2008) Spectroscopic studies of kaolin from different Brazilian regions. *Clay Miner* 43(1):129–135
- BS1377-7 BS- (2003) Code of practice for soil engineering purposes: Shear strength tests (total stress). British Standards Institution, Milton, UK
- Sridharan A, Sivapullaiah PV (2005) Mini compaction test apparatus for fine grained soils. *Geotech Test J* 28(3):1–7
- Assaad JJ, Harb J (2012) Use of the falling-head method to assess permeability of freshly mixed cementitious-based materials. *J Mater Civ Eng* 25(5):580–588
- Chorom M, Rengasamy P (1995) Dispersion and zeta potential of pure clays as related to net particle charge under varying pH, electrolyte concentration and cation type. *Eur J Soil Sci* 46(4):657–665
- Jones JB Jr (2001) Laboratory guide for conducting soil tests and plant analysis. CRC Press, Boca Raton
- Heil D, Sposito G (1993) Organic matter role in illitic soil colloids flocculation: II. Surface charge. *Soil Sci Soc Am J* 57(5):1246–1253
- Lorenz PB (1969) Surface conductance and electrokinetic properties of kaolinite beds. *Clays Clay Miner* 17(4):223–231
- Stevenson FJ (1994) Humus chemistry: genesis, composition, reactions. Wiley, New York
- Van Olphen H, Hsu PH (1978) An Introduction to Clay Colloid Chemistry. *Soil Sci* 126(1):59
- Sridharan A, Rao GV (1973) Mechanisms controlling volume change of saturated clays and the role of the effective stress concept. *Geotechnique* 23(3):359–382
- Kamon M, Ying C, Katsumi T (1997) Effect of acid rain on physico-chemical and engineering properties of soils. *Soils Found* 37(4):23–32
- Bell FG (2013) Fundamentals of engineering geology. Elsevier, Amsterdam
- Moh Z-C, Mazhar MF (1900) Effects of method of preparation on index properties of lateritic soils. Paper presented at the Soil Mech & Fdn Eng Conf Proc/Mexico
- Ola S (1978) Geotechnical properties and behaviour of some stabilized Nigerian lateritic soils. *Q J Eng GeolHydrogeol* 11(2):145–160